Retina

Direct Tie2 Agonists Stabilize Vasculature for the Treatment of Diabetic Macular Edema

Nicholas J. Agard[1,*], Gu Zhang[1,*], John Ridgeway[1], Danielle M. Dicara[1], Phillip Y. Chu[1], Rachana Ohri[1], Sarah Sanowar[1], Jean-Michel Vernes[1], Hannah Chi[1], Jiameng Zhang[1], Emily Holz[1], Maciej Paluch[1], Guannan He[1], Yingjia Benson[1], Jianhuan Zhang[1], Pamela Chan[1], Nga Tang[1], Prachi Javale[1], Blair Wilson[1], Kathy Barrett[1], Rebecca K. Rowntree[1], Julie Hang[1], Y. Gloria Meng[1], Phil Hass[1], Germaine Fuh[1], Robert Piskol[1], Vladimir Bantseev[1], Kelly M. Loyet[1], John C. Tran[1], Cong Wu[1], Vahan B. Indjeian[1], Vittal Shivva[1], and Minhong Yan[1]

[1] Genentech Research and Early Development, South San Francisco, CA, USA

Purpose: Diabetic macular edema (DME) is the leading cause of vision loss and blindness among working-age adults. Although current intravitreal anti-vascular endothelial growth factor (VEGF) therapies improve vision for many patients with DME, approximately half do not achieve the visual acuity required to drive. We therefore sought additional approaches to resolve edema and improve vision for these patients.

Methods: We explored direct agonists of Tie2, a receptor known to stabilize vasculature and prevent leakage. We identified a multivalent PEG–Fab conjugate, Tie2.1-hexamer, that oligomerizes Tie2 and drives receptor activation and characterized its activities in vitro and in vivo.

Results: Tie2.1-hexamer normalized and stabilized intercellular junctions of stressed endothelial cell monolayers in vitro, suppressed vascular leak in mice under conditions where anti-VEGF alone was ineffective, and demonstrated extended ocular exposure and robust pharmacodynamic responses in non-human primates.

Conclusions: Tie2.1-hexamer directly activates the Tie2 pathway, reduces vascular leak, and is persistent within the vitreal humor.

Translational Relevance: Our study presents a promising potential therapeutic for the treatment of DME.

1

Introduction

Approximately 442 million people worldwide have diabetes mellitus.[1,2] Of these, about 21 million have progressed to diabetic macular edema (DME), the leading cause of vision loss and blindness among adults 20 to 72 years old.[3–6] The etiology of DME-associated vision loss is partially understood. Diabetes-associated hyperglycemia and hyperlipidemia drive complex physiological changes in the retinal microvasculature, resulting in abnormal or reduced vascular flow and increased permeability.[7,8] Prolonged exposure to these conditions can drive both damage to retinal endothelial cells and disruption of the blood–retinal barrier, resulting in macular edema. Furthermore, retinal neovascularization often occurs in response to the closure or non-perfusion of existing capillaries.[9] Unfortunately, the new vessels are often leaky, worsening the accumulation of interstitial retinal fluid that is characteristic of DME.

Anti-vascular endothelial growth factor (VEGF) agents, such as ranibizumab (Lucentis; Genentech, Inc., South San Francisco, CA) and aflibercept (Eylea; Regeneron Pharmaceuticals, Tarrytown, NY), are approved intravitreal biologics for the treatment of DME.[10] Inhibition of VEGF signaling suppresses weakening of endothelial cell junctions and prevents vascular leakage.[11] In the pivotal RISE and RIDE phase III clinical trials in patients with DME, monthly intravitreal treatment with ranibizumab drove substantial improvements (>15 letters) in 45% of patients and corresponding drying of macular edema.[12] Despite these impressive gains, a significant percentage of patients failed to achieve normal vision or corrected eyesight sufficient to operate an automobile (20/40 vision), suggesting that treatment with anti-VEGF alone does not address all of the pathways underlying DME pathology. Furthermore, the frequency of intravitreal injections in the trials (every 4–8 weeks) is often poorly adhered to in clinical practice, resulting in undertreatment and associated vision loss.[13] Although pro re nata treatment or medical devices can successfully extend the dosing interval of anti-VEGF treatments for some patients with DME, treatment durability remains of paramount concern for intravitreal DME treatments.[14,15]

Faricimab, an intravitreally administered anti-VEGF/angiopoietin 2 (Ang-2) bispecific antibody, was developed to address the substantial remaining unmet need of patients with DME by targeting multiple pathways.[16,17] Ang-2 is a context-dependent antagonist/partial agonist of the receptor tyrosine kinase Tie2 and agonist of β1 integrin.[18,19] In response to inflammatory signals, the expression of Ang-2 is elevated.[20,21] Ang-2 competes against the Tie2 agonist ligand angiopoietin 1 (Ang-1) and compromises optimal Tie2 signaling, synergizing with integrin signaling to destabilize cell–cell junctions and increase vascular leakage. Inhibition of Ang-2 in the retina of patients with DME is thought to promote Tie2 signaling through its native ligand, Ang-1.[22] The YOSEMITE and RHINE phase III clinical trials showed that treatment with faricimab reduced macular edema and provided durable vision improvement, as over 60% of patients achieved a dose interval of every 16 weeks at 2 years.[23,24] These data provided the foundation for the recent U.S. Food and Drug Administration approval of faricimab as Vabysmo (Genentech) and highlights the importance of the Ang-2/Tie2 pathway.

Alternative agents have been explored to enhance Tie2 signaling, including small-molecule inhibition of vascular endothelial protein tyrosine phosphatase (VE-PTP), a phosphatase that inactivates Tie2.[25–27] VE-PTP inhibitors prevent inactivation of basal Tie2 signaling but do not directly catalyze phosphorylation of the kinase. Unlike the aforementioned indirect approaches to Tie2 activation, we considered direct Tie2 agonism as a way to drive pathway activation. Here, we describe the development of a multivalent Tie2 agonist with desirable activity and drug profile.

Methods

In Vivo Studies

Animals used in these studies were maintained in Association for Assessment and Accreditation of Laboratory Animal Care-accredited animal facilities. The local animal care committees, in accordance with the ARVO Statement for the Use of Animals in Ophthalmic and Vision Research, approved all animal protocols.

DNA and Protein Design and Production

All antibodies in this work are numbered using Eu numbering systems for constant domains and Kabat numbering for variable domains.[28,29] Antibody constructs were generated by gene synthesis (GENEWIZ; Azenta Life Sciences, Chelmsford, MA) or through mutagenesis using the Q5 Site-Directed Mutagenesis Kit (New England Biolabs, Ipswich, MA). Recombinant proteins and antibodies, including those containing cysteine mutations, were produced by transient transfection of Chinese hamster ovary

cells with recombinant DNA and purified by affinity chromatography. Recombinant Fabs for conjugation were generated in *Escherichia coli*. The FLAG-tagged Tie2 extracellular domains were expressed and purified from CHO cell-conditioned media. After 11 to 14 days, the conditioned media were harvested and concentrated approximately tenfold. The concentrate was affinity purified by affinity purification (ANTI-FLAG M2 Affinity Gel; Sigma-Aldrich, St. Louis, MO) followed by size-exclusion column (either Superdex 200 or Superdex 75; Sigma-Aldrich).

Generation of Anti-Tie2 Antibodies

Antibodies binding the extracellular domain of Tie2 were selected from phage-displayed synthetic antibody libraries that were built on the trastuzumab framework by introducing synthetic diversity at solvent-exposed positions within the heavy-chain complementarity-determining regions.[30] The phages were selected for binding to plate-bound Tie2 antigens (5 µg/mL) over four rounds of panning.

Generation of Anti-Tie2 Multimers

Purified Fab was reduced and partially reoxidized in preparation for conjugation essentially as previously described.[31] Fabs were conjugated to polyethylene glycol (PEG) multimers (JenKem Technology, Plano, TX) in 25-mM sodium acetate (pH 6.5), 150-mM sodium chloride, and 4-mM EDTA, at a concentration around 5 mg/mL. Following equilibrating to room temperature, PEG–maleimide multimer was resuspended in 25-mM sodium acetate (pH 5.0) to a concentration of 10 mg/mL. Upon solubilization, PEG was added to the Fab pool, maintaining a slight excess of Fab for each maleimide ON (overnight). Following conjugation, the hexamer was purified using size-exclusion chromatography on a Sephacryl S-300 HR column (GE Healthcare, Chicago, IL) in 20-mM His-acetate (pH 5.5) and 50-mM sodium chloride followed by cation exchange using SP Sepharose High Performance strong cation exchange resin from GE Healthcare to enrich for the desired conjugate. The cation exchange step was run in 25-mM sodium acetate (pH 5.0) and eluted using a 10% to 20% 1-M sodium chloride gradient over 50 column volumes. For all processes, the Fab/PEG ratio was determined by size-exclusion chromatography using a 300-mm × 8-mm Shodex OHpak SB-804 HQ run (Showa Denko, Tokyo, Japan) at 0.8 mL/min using phosphate-buffered saline (PBS; pH 7.2) and 150-mM sodium chloride under isocratic conditions.

Monitoring of Human Vascular Endothelial Cell or Rat Aortic Endothelial Cell Phospho-AKT by Fluorescence Resonance Energy Transfer

Tie2 stimulation was monitored by tracking phosphorylation of the downstream substrate AKT by western blot or homogeneous time-resolved fluorescence (HTRF) in human vascular endothelial cells (HUVECs; Lonza, Basel, Switzerland) or rat aortic endothelial cells (RAECs). HUVECs were trypsinized and seeded into sterile 96-well plates at 0.4×10^5 cells/well in 100-µL culture medium (Media MCDB-131 Complete; VEC Technologies, Rensselaer, NY), and the plates were incubated in a 37°C, 5% CO_2 incubator overnight. The culture medium was removed, and 100 µL pre-warmed serum starvation media (EndoGRO Basal Medium; MilliporeSigma, Burlington, MA) was added into each well of the plates. The plates were incubated in a 37°C, 5% CO_2 incubator for 3 hours prior to incubation with the anti-Tie2 antibodies. RAECs were seeded at a density of 12,000 cells/well in 96-well cell culture plates and cultured in 100-µL EGM-2MV Microvascular Endothelial Cell Growth Medium (Lonza) overnight at 37°C with 5% CO_2. After overnight culture, the cells were starved in EBM Endothelial Cell Growth Basal Medium (Lonza) with 0.1% BSA for 3 hours prior to incubation with the anti-Tie2 antibodies.

Tie2 agonists were diluted to an initially high stock concentration (typically 30–1000 µg/mL) in assay buffer followed by serial dilution (typically 2- to 10-fold). These dilutions (50 µL) were added to each well after removal of the serum starvation media, and the plates were incubated at 37°C with 5% CO_2 for 15 minutes. The solution was removed, and 50 µL of lysis buffer containing blocking buffer from a Phospho-AKT1/2/3 (Ser473) Cellular Kit (Cisbio, Codolet, France) was added to cells. The plates were incubated at room temperature protected from ambient light for about 30 to 45 minutes with gentle shaking and kept at −80°C until used, or they were directly used in HTRF assays per the manufacturer's instructions. The data were calculated as the ratio of the acceptor and donor emission signals times 10^4 for each individual well.

For testing the effects of cross-linking anti-Tie2 antibodies, 20 µg/mL polyclonal goat anti-hIgG was used as the crosslinker (Jackson ImmunoResearch Laboratories, Inc., West Grove, PA). Assay buffer (Lonza Basal Medium + 0.2% BSA) was mixed with an equal volume of anti-Tie2 bivalent antibody at 60 µg/mL and incubated at room temperature for 1 hour.

After incubation, the mixture was subjected to a three-fold serial dilution and added to the serum-starved cells, and the assay proceeded as described above.

For measuring active Tie2.1-hexamer concentrations in cyno vitreous samples, HUVEC-based phospho-AKT (pAKT) assays were used. Cells were seeded at 20,000/well in 96-well plates. The standard curve range was 6.3 to 400 ng/mL with a reporting range of 12.5 to 200 ng/mL. The minimum sample dilution was 1:100. The assay detection limit was 1.2 µg/mL for vitreous samples.

Western Blot Analysis for pAKT or Tie2

HUVEC cells were plated at 1×10^6 cells per well in EndoGRO Medium and cultured at 37°C for 16 to 18 hours. Culture medium was changed to 0.1% BSA EndoGRO Basal Medium for 4 to 5 hours prior to stimulation. Cells were incubated with the relevant Tie2 agonists for 30 minutes at 37°C and washed three times with cold PBS (pH 7.4). Cells were placed on ice and incubated with 100 µL/well of radioimmuno-precipitation assay (RIPA) buffer (Sigma-Aldrich) containing Roche complete protease and phosphatase inhibitors (Thermo Fisher Scientific, Waltham, MA) for 5 minutes. Lysates were harvested from wells using a cell scraper and centrifuged at 17,800g for 10 minutes. Supernatant was assessed by sodium dodecyl sulfate–polyacrylamide gel electrophoresis (SDS-PAGE; 8% NuPAGE Bis-Tris; Thermo Fisher Scientific), followed by transfer to a nitrocellulose membrane. Membranes were blocked with 5% BSA in Tris-buffered saline with Tween 20 (TBST) for 1 hour at room temperature and probed with rabbit anti-pAKT (Cell Signaling Technology, Danvers, MA) in blocking buffer. Following four washes with TBST, membranes were probed with horseradish peroxidase (HRP) anti-rabbit immunoglobulin (1:10,000; GE Healthcare) at room temperature for 1 hour. Membranes were washed three times with TBST and incubated with chemiluminescence reagents (Thermo Fisher Scientific) at room temperature for 5 minutes prior to exposing blots to film.

For anti-Tie2 blots, cells were grown on EndoGRO Medium in the presence of agonist for 18 to 20 hours and lysed on ice in 100 µL RIPA buffer (Sigma-Aldrich) supplemented with a cocktail of protease inhibitor and phosphatase inhibitors (Thermo Fisher Scientific). Cell lysates were centrifugated at 14,000 rpm at 4°C for 10 minutes before being subjected to anti-Tie2 western blot (WB) analysis. A standard WB analysis was performed using a mouse anti-Tie2 primary antibody (BD, Franklin Lakes, NJ) and a secondary detecting antibody (HRP anti-mouse IgG; GE Healthcare).

Tie2 Degradation In Vivo

To assess the effects of anti-Tie2 antibodies on Tie2 levels in an in vivo assay, 8- to 9-week-old C57BL/6 mice (Charles River Laboratories, Wilmington, MA) were dosed with Tie2 agonist at 20 mg/kg via intraperitoneal injection. Mice were euthanized under CO_2 at different time points after anti-Tie2 antibody administration. Mouse lung tissues were dissected out and stored at −80°C after snap freezing. About 20 mg of mouse lung tissue was homogenized in 1 mL of ice-cold RIPA buffer (Sigma-Aldrich) containing a cocktail of proteinase and phosphatase inhibitors (Thermo Fisher Scientific). After clarification by centrifugation, tissue lysates were subjected to WB analysis using mouse anti-Tie2 (BD) together with HRP anti-moue IgG Ab (GE Healthcare) as secondary detecting antibody. The WB membrane was developed using Thermo Scientific chemiluminescence reagents (Thermo Fisher Scientific).

Monolayer Permeability Assay

A HUVEC permeability assay was used to measure the endothelial cell (EC) leakage of a presently disclosed anti-Tie2 agonistic antibody, Tie2.1. HUVEC cells (MilliporeSigma) were seeded at 0.1×10^6 per well of 24-well plates (Sigma-Aldrich) in complete EndoGRO Medium. Three days later, culture medium was changed to EndoGRO Basal Medium followed by 16 hours of incubation. Then, agonistic Tie2 antibodies (10 µg/mL) were added. After an incubation of 30 minutes, 50 µL of 5-mg/mL FITC–dextran (Sigma-Aldrich) was added into each insert, and 50 µL of medium was taken from the receiver tray of each well at different time points and measured by a microplate reader (excitation filter, 485 nm; emission filter, 535 nm).

Immunofluorescence

EndoGRO HUVEC cells (MilliporeSigma) were seeded at 0.2×10^6 per well on 4-well chamber slides in complete EndoGRO Medium. Three days later, culture medium was changed to EndoGRO Basal Medium. After an incubation of 3 hours, 1 or 10 µg/mL Tie2 agonistic antibodies was added. After antibody treatment, cells were washed three time with ice-cold PBS and fixed with 3% paraformaldehyde (Electron Microscopy Sciences, Hatfield, PA) at room temperature for 20 minutes. Fixed cells were washed three times

with ice-cold PBS and permeabilized with 0.1% PBS–Triton (PBST) at room temperature for 10 minutes. After blocking with blocking buffer (10% normal donkey serum + PBS + 0.1% Triton X-100) for 1 hour at room temperature, cells were incubated with mouse anti-human VE-cadherin (BD) at a dilution of 1:250 overnight at 4°C. Invitrogen Alexa Fluor 633 Phalloidin (Thermo Fisher Scientific) was used for F-actin staining. Slides were washed with PBST five times at room temperature and then incubated with Alexa Fluor 549 donkey anti-mouse IgG (H+L) (Jackson ImmunoResearch), 1:500 dilution, for 2 hours at room temperature in the dark. Slides were washed four times with PBST and then two times with PBS at room temperature. Slides were then stained with 4′,6-diamidino-2-phenylindole (DAPI; Sigma-Aldrich) at a 1:10000 dilution of 5 mg/mL for 10 minutes at room temperature. They were then mounted with Invitrogen Prolong Gold antifade reagent. Fluorescence images were obtained using confocal microscopy (Leica Camera, Wetzlar, Germany).

In Vivo Vascular Permeability Assay

Balb/c mice (Charles River Laboratories), 5 to 8 weeks old, were dosed with 1% of Evans Blue (Sigma-Aldrich) was given via intravenous injection. Ten minutes later, the mice were anesthetized under isoflurane, and anti-VEGF G6.31 or Tie2 agonist hexamer PEG Fab2.1 together with VEGF (produced in house) were injected intradermally into the mouse ears. Thirty minutes later, mice were euthanized by CO_2, and the mouse ears were excised. Evans Blue that had extravasated into the ear tissues was extracted with formamide (Sigma-Aldrich) and quantified spectrophotometrically at 620 nm and 760 nm.

Monkey Pharmacokinetic and Pharmacodynamic Analyses

Nonclinical studies with cynomolgus monkeys were performed to assess the exposure, stability, and activity of the therapeutic candidates. Naïve male cynomolgus monkeys of 2 to 4 kg body weight and approximately 2 to 4 years of age were assigned to dose groups. Potential therapeutics were administered via a single 50-μL intravitreal injection (2-mg dose) in both eyes of anesthetized monkeys, and they were observed for up to 21 days. Doses were administered by a board-certified veterinary ophthalmologist at approximately the 7 o'clock position to the right eye and the 5 o'clock position to the left eye. Clinical ophthalmic examinations (slit-lamp biomicroscopy and indirect ophthal-moscopy) were performed throughout the study by a board-certified veterinary ophthalmologist. After intravitreal dosing, at predetermined time points, animals were euthanized (two animals per group per time point) for the collection of ocular samples (vitreous and aqueous humor). Blood samples were also collected from all surviving animals in serum separator tubes. All serum samples were stored at −70°C until they were assayed for drug concentrations or Ang-2 levels.

ELISA of Anti-Tie2 Hexamers

Concentrations of anti-Tie2 Fab hexamers were determined with an anti-Tie2 ELISA. Nunc MaxiSorp 384-well plates (Nalge Nunc International, Rochester, NY) were coated with 1 μg/mL recombinant human Tie2 (Abcam, Cambridge, UK) diluted in coating buffer (50-mM carbonate/bicarbonate buffer, pH 9.6) and incubated overnight at 4°C. The plates were washed three times with wash buffer (PBS, pH 7.4, and 0.05% Tween 20) and treated with blocking buffer (PBS, 0.5% BSA, and 15-ppm Proclin, pH 7.4) for 2 hours at room temperature. The plates were washed three times with wash buffer, and samples diluted in sample diluent (PBS, 0.5% BSA, 0.05% Tween 20, 5-mM EDTA, 0.25% CHAPS, 0.35-M NaCl, and 15 ppm Proclin, pH 7.4) were added to the wells and incubated at room temperature for 2 hours. The plates were washed six times with wash buffer. The detection antibody (goat anti-human IgG H+L–HRP; Bethyl Laboratories, Montgomery, TX) was then diluted to 100 ng/mL in detection buffer (PBS, 0.5% BSA, 0.05% Tween 20, and 15 ppm Proclin, pH 7.4) and added to the wells and incubated on a shaker for 1 hour at room temperature. The plates were washed six times with wash buffer and developed using 3,3′,5,5′-tetramethylbenzidine (TMB) peroxidase according to the manufacturer's instructions. The reportable assay range was 0.31 to 10 ng/mL (lower limit of quantitation was 6 ng/mL for monkey serum and 31 ng/mL for vitreous and aqueous humor). The concentrations of anti-Tie2 Fab hexamers shown in Figure 5a were similarly determined with a generic human IgG ELISA using sheep anti-human IgG (monkey adsorbed; The Binding Site, San Diego, CA) for coating. The minimum detection limit was 2.4 ng/mL for serum samples. Vitreous and aqueous humor samples were diluted at least 1:100 and showed good linearity in serial dilution with a small percent coefficient of variation. Minimum dilution was not determined due to lack of blank vitreous and aqueous humor samples. Pharmacokinetic analyses of concentration–time data across

matrices was performed using a non-compartmental analysis method (Phoenix WinNonlin 6.4; Pharsight Corp., Mountain View, CA) with nominal time and dose.

RNA-Sequencing and Analysis

Cultured human retinal microvascular endothelial cells were treated with PBS or Tie2.1-hexamer and harvested at 4 and 24 hours. Total RNA was extracted using the RNeasy Micro-Kit (QIAGEN, Hilden, Germany). Three replicate samples were collected for each treatment condition. The concentration of RNA was determined using the NanoDrop 8000 spectrophotometer (Thermo Fisher Scientific), and the integrity of RNA was determined using Fragment Analyzer (Advanced Analytical Technologies, Ankeny, IA). Approximately 500 ng of total RNA was used as an input for library preparation using the TruSeq RNA Sample Preparation Kit v2 (Illumina, San Diego, CA). The size of the libraries was confirmed using the High Sensitivity D1000 Screen Tape System (Agilent Technologies, Santa Clara, CA), and their concentration was determined by a quantitative PCR-based method using a KAPA Library Quantification Kit (Roche, Basel, Switzerland). The libraries were multiplexed and sequenced on an Illumina HiSeq 4000.

Reads were first aligned to ribosomal RNA sequences to remove ribosomal reads. The remaining reads were aligned to the human reference genome (NCBI Assembly GRCh38) using GSNAP[32] (version 2013-10-10), allowing a maximum of two mismatches per 50 base-pair sequence (parameters: '-M 2 -n 10 -B 2 -i 1 -N 1 -w 200000 -E 1 –pairmax-rna=200000 –clip-overlap'). Transcript annotation was based on the human RefSeq database NCBI Annotation Releases 106. To quantify gene expression, the number of reads mapped to the exons of each RefSeq gene was calculated using the HTSeqGenie R package (R Foundation for Statistical Computing, Vienna, Austria). Read counts were scaled by library size and quantile normalized, and precision weights were calculated using the voom R package.[33] Subsequently, differential expression analysis on the normalized count data was performed using the limma R package[34] by contrasting Tie2.1-hexamer–treated samples with control samples. Gene expression was considered significantly different across groups if we observed a |log2-fold change| $\geq$ 1 (estimated from the model coefficients) associated with a false discovery rate–adjusted $P \leq$ 0.05. In addition, gene expression was obtained in the form of normalized reads per kilobase of transcript per million mapped reads (nRPKM) as described previously.[35]

Capillary Electrophoresis–SDS–Laser-Induced Fluorescence of Anti-Tie2 Multimers

Samples were prepared using a protocol reported previously with minor modifications.[36] Briefly, vitreous humor samples were first mixed with sodium phosphate at pH 6.7 at a volume ratio of 1:1. Then, 4% SDS with 150-mM N-ethylmaleimide was added to the sample mixture, which was incubated at 70°C for 5 minutes. After the mixture was cooled to room temperature, 3-(2-furoyl) quinolone-2-carboxaldehyde dye (Thermo Fisher Scientific) was added followed by the addition of potassium cyanide. The sample mixture was then incubated at 50°C for 10 minutes. After cooling to room temperature, the samples were loaded onto a PA 800 Plus Pharmaceutical Analysis System capillary electrophoresis (CE) instrument (Sciex, Framingham, MA). The CE–SDS–laser-induced fluorescence (LIF) method has been described previously.[36,37] For LIF detection, the excitation wavelength was 488 nm and the detection wavelength was 600 nm. The intact hexamer peak and the degradant pentamer peak were quantified using the integrated peak areas.

Determination of Anti-Tie2 Oxidation

Detection and quantitation of oxidation present at the amino acid residue level of anti-Tie2 constructs were performed as follows. First, 40 µL biological matrix (e.g., vitreous humor) containing the anti-Tie2 construct was mixed with 80 µL of denaturing solution (8-M urea, 25-mM 1,4-dithiothreitol, and 100-mM ammonium bicarbonate, all solubilized in water). The mixture was incubated at 25°C for 30 minutes. Then, 10 µL of 500-mM iodoacetamide was added to the mixture, which was then incubated for 30 minutes at 25°C in the dark. This was followed by adding 10 µL Asp-N (Promega, Madison, WI) at a concentration of 0.1 mg/mL (in water) to the mixture. Additionally, 180 µL of water was added to the mixture. The mixture was then incubated at 37°C for 1 hour, followed by the addition of 10 µL Trypsin/Lys-C Mix (Promega) at a concentration of 0.2 mg/mL (in water) to the mixture. The mixture was incubated at 37°C for 3 hours, after which 35 µL of the mixture was injected onto a Waters nanoACQUITY UPLC System (Waters Corporation, Milford, MA) coupled to a Thermo Scientific Orbitrap Elite MS (Thermo Fisher Scientific). The raw data collected were then analyzed using Thermo Fisher Scientific BioPharma Finder software, which allowed identifying modifications (e.g., oxidation) at the amino acid level through a combination of high-resolution mass data and collision-induced dissociation (CID)

fragmentation data. Specifically, oxidation was identified by observing mass shifts of +16 Da (or an integer multiple); the specific location was determined through peptide sequencing using tandem mass spectrometry (CID fragmentation mode). Furthermore, methionine oxidation was confirmed by observing characteristic −64-Da mass shifts after CID fragmentation. Quantitation was determined via mass spectrometry by dividing ion intensities associated with oxidized species by the ion intensity of naïve (unoxidized) species.

Plasma Levels of Ang-2 After Intravitreal Administration of a Tie2 Agonist

Plasma from the cynomolgus monkeys administered agonists was assayed to determine systemic levels of Ang-2 at various time points after administration. Cynomolgus monkey plasma samples were analyzed by ELISA developed using a DuoSet Human Angiopoietin 2 ELISA Development Kit (R&D Systems, Minneapolis, MN). A mouse antibody was used for capture. Bound Ang-2 was detected using a biotinylated mouse antibody, followed by HRP-conjugated streptavidin (GE Healthcare) and 3,3′,5,5″-tetramethylbenzidine (Moss Biotech, Severn, MD) as substrate. The minimum plasma dilution was 1:10 in the sample diluent (PBS, 0.5% BSA, 0.05% Tween 20, 10-ppm Proclin 300, 0.25% CHAPS, 5-mM EDTA, and 0.35-M NaCl), and the detection limit for this assay was 120 pg/mL in plasma.

Results

Development of Tie2 Agonists

To investigate whether direct activation of Tie2 could stabilize vasculature and reduce macular edema, we sought to generate a Tie2 agonist. We generated more than 400 anti-Tie2 antibodies from a combination of phage display, hybridoma, and single B-cell technologies. Binders were characterized to identify antibodies with agonist potential by measuring their ability to drive pAKT signaling downstream of Tie2 in UVECs and RAECs. Clone Tie2.1 initially emerged as a promising agonist; however, further study revealed that the level of agonistic activity of Tie2.1 hIgG1 depends on low levels of protein aggregate (Supplementary Fig. S1a). Interestingly, cross-linking with polyclonal anti-human IgG antibody conferred potent agonist activity to a highly purified preparation of Tie2.1 (Supplementary Figs. S1a, S1b). Our findings

are consistent with reports that Tie2 activation relies on multivalent ($n > 2$) Tie2 clustering.[38]

We further characterized Tie2.1 as a potential lead. Tie2.1 bound human, cynomolgus monkey, mouse, and rat Tie2 with modest (micromolar) monovalent affinities and competed with both Ang-1 and Ang-2 for binding (Supplementary Fig. S1c). We also characterized two additional antibodies from the antibody campaign, Tie2.20 and Tie2.38 (Supplementary Fig. S1c). Although Tie2.20 also competes with the native ligands for Tie2 binding, Tie2.38 is a non-blocking antibody. Notably, cross-linking of either Tie2.20 or Tie2.38 failed to induce Tie2 signaling, indicating an apparent requirement for epitope-specific multivalent engagement.

Given the strong agonist potential of Tie2.1 when in an aggregate format, we decided to explore multivalent molecular formats intended to drive clustering of Tie2. We conjugated Tie2.1 Fabs to PEG scaffolds of various valency and length to identify the optimal molecular design of a Tie2 agonist (Fig. 1a). We found that the activity of the PEG conjugates increased with higher valency (six or eight binders) and shorter arm length (Fig. 1b), suggesting that the density of Tie2 clustering is a determinant of signaling strength. In the current study, we focused on Tie2.1-hexamer, a 6-kDa PEG hexamer conjugated with Tie2.1 Fab resulting in a 295-kDa conjugate. The apparent dependence on clustering seen in Figure 1b predicted that supersaturation of Tie2 with Tie2.1-hexamer could lead to reduced Tie2 clustering and signaling. Indeed, in a dose-ranging in vitro experiment, we observed a clear bell-shaped activity curve (Fig. 1c), with a loss of 50% of maximal activity occurring at approximately 100 µg/mL of Tie2.1-hexamer (∼2 µM of total Fab). Given the low monovalent affinity of Tie2.1 and the Ang-1/-2 competitive nature of binding, we sought to characterize whether the hexamer would continue to activate Tie2 in the presence of Ang-2, which can expressed during DME. Although excess Ang-2 could partially reduce the activity of Tie2.1-hexamer, equimolar concentrations of the agonist appeared to fully agonize the kinase (Supplementary Fig. S2).

As an alternative approach to generating Tie2 agonist, we recombinantly expressed a biparatopic Fab-IgG intended to enable more extended clustering on the cell surface with the potential for greater signaling (Fig. 1a).[39,40] We found that the biparatopic Tie2.1.38 (comprised of two copies of the Fabs from both Tie2.1 and Tie2.38) drove Tie2 signaling comparable to the level induced by recombinant Ang-1 (Fig. 1b). Next, we carried out dose–response studies for both molecules, evaluated at both 15-minute and 24-hour time points (Fig. 1d). At 15 minutes,
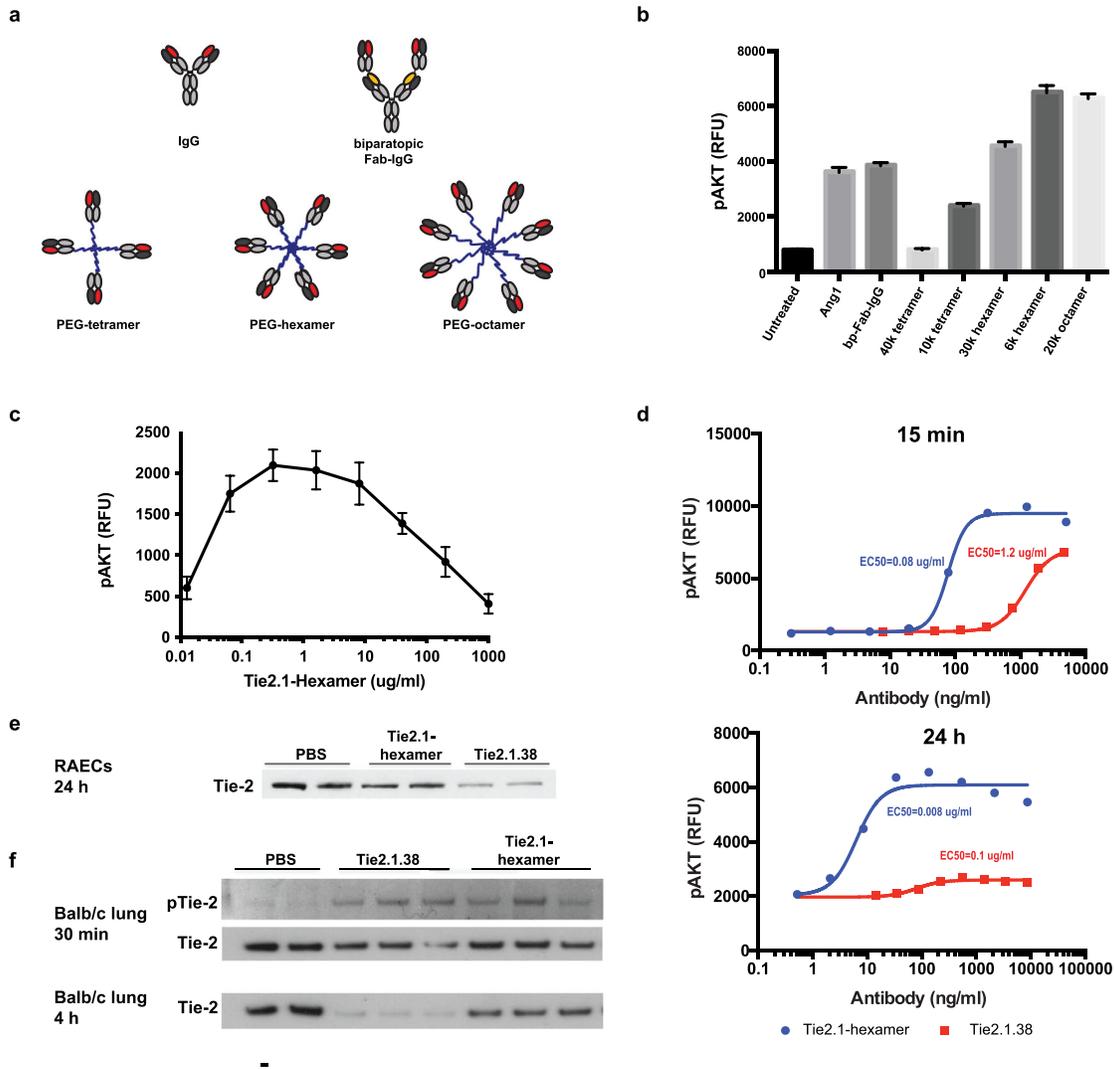
Figure 1. Development of Tie2 agonists driving strong and persistent Tie2 signaling. (a) Illustration of Tie2 agonist structures. (b) RAECs treated with 100 ng/mL of Ang-1 or 10 µg/mL of indicated agonists for 15 minutes were evaluated for pAKT levels using HTRF. (c) Dose response of Tie2.1-hexamer as determined by pAKT levels at 15 minutes. (d) Dose response of Tie2.1-hexamer and Tie2.1.38 Fab-IgG at 15 minutes and 24 hours as determined by pAKT levels. (e) Western blot analysis of total Tie2 levels following 24-hour treatment with 10 µg/mL indicated agonists. (f) Western blot analysis of total Tie2 and phospho-Tie2 in lung tissue of Balb/C mice 30 minutes and 4 hours following 10-mg/kg administration of agonist. Data shown in (b) and (c) are mean ± SD ($n = 3$), and data shown in (d) are mean ± range ($n = 2$).

the Tie2.1-hexamer was ∼15-fold more potent but led to a maximum pAKT signal similar to that of Tie2.1.38. At 24 hours, both molecules showed ∼10-fold improvements in potency. Interestingly, although the Tie2.1-hexamer showed a modest (<twofold) reduction in maximal signaling upon extended exposure, Tie2.1.38 showed an ∼10-fold reduction at 24 hours.

To understand the difference in signaling duration between Tie2.1-hexamer and Tie2.1.38, we measured Tie2 protein levels in RAECs at 24 hours after stimulation. The results showed that Tie2.1.38 induced

substantial Tie2 depletion, whereas the Tie2.1-hexamer left the receptor largely intact (Fig. 1e). We further investigated Tie2 downregulation in vivo. Intraperitoneal administration of both molecules into Balb/c mice confirmed induction of Tie2 signaling as measured by pTie2 levels in lung tissue at 30 minutes. Again, compared with Tie2-hexamer, Tie2.1.38 induced more substantial target depletion by 4 hours after antibody injection (Fig. 1f). Together, these studies indicate that Tie2.1-hexamer can promote more persistent and potent signaling than Tie2.1.38, and it was thus pursued as a clinical candidate.
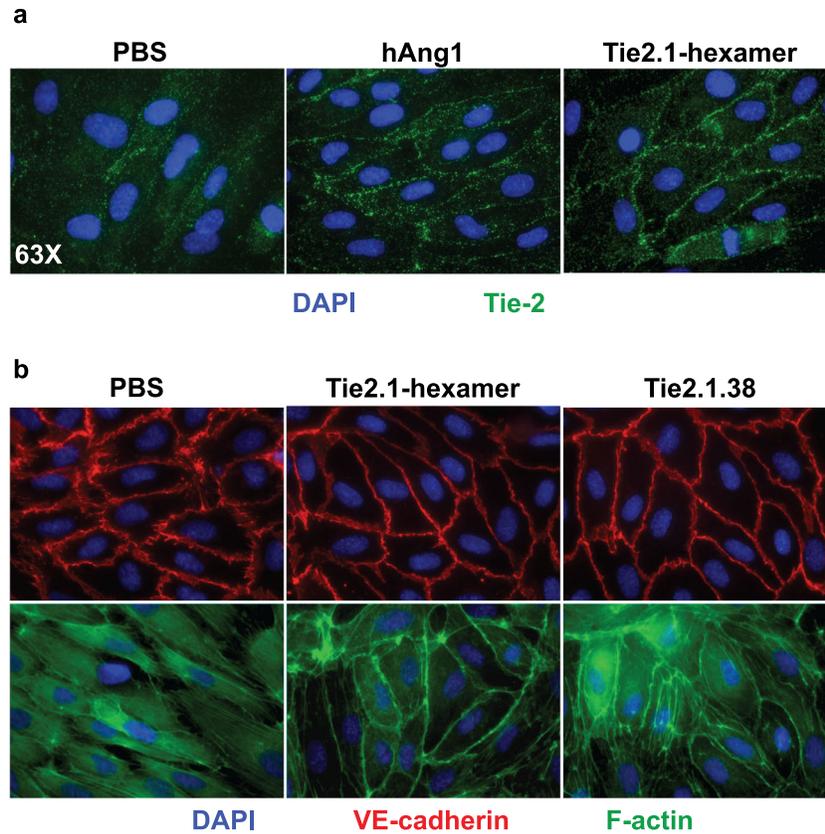
Figure 2. Tie2 agonists stabilize cellular junctions. (a) Immunofluorescence imaging of HUVEC cells treated with 100 ng/mL of Ang-1 or 10 µg/mL of Tie2.1-hexamer for 3 hours and stained with DAPI (*blue*) or anti-Tie2 (*green*). (b) Tie2 agonists drove relocalization to cell–cell contacts. HUVEC cells treated as above or with 10 µg/mL of Tie.1.38 Fab-IgG were stained with DAPI (*blue*), anti-VE-cadherin (*red*), or phalloidin (*green*) and analyzed by fluorescent microscopy.

Functional Assessment of Tie2 Agonists

Consistent with a previous study of Ang-1, treatment of HUVECs with the Tie2.1-hexamer drove translocation of Tie2 to cell–cell contacts (Fig. 2a).[40] Immunofluorescent analysis showed that stimulation with Tie2 agonists resulted in an increase in junctional VE-cadherin and cortical actin (Fig. 2b), indicating reinforced endothelial cell–cell junctions. To assess the functional consequences of Tie2 agonism, we looked at the impact of the Tie2.1-hexamer on endothelial cell barrier integrity. Well-formed monolayers of HUVECs were subjected to serum starvation to compromise the cell–cell junctions, resulting in the apparent transit of FITC-labeled dextran through the monolayer of cells (Fig. 3a). We found that either Tie2.1-hexamer or Ang-1 substantially reduced the leak, likely reflecting both pro-survival phosphatidylinositol-3-kinase signaling and endothelial junction tightening induced downstream of Tie2. In contrast, treatment with two different Ang-2–specific blocking antibodies worsened permeability, presum-

ably reflecting the partially agonistic activity of Ang-2 under conditions where Ang-1 is low or absent (Supplementary Fig. S3).[41]

To demonstrate the agonistic activity of the Tie2.1-hexamer in vivo, we used a modified version of the Miles assay in BALB/c mice wherein dermal vascular leakage was assessed following the coadministration of an inducer of vascular leak (VEGF or lipopolysaccharide [LPS]) and a therapeutic agent into the ears.[42] As expected, VEGF treatment alone resulted in substantial vascular permeability (Fig. 3b). This effect was effectively suppressed by a VEGF-blocking antibody or the Tie2.1-hexamer. Next, we utilized LPS as a pleiotropic inducer of vascular leak, potentially better reflecting the mixture of inflammatory signaling present in DME.[43] LPS is also reported to reduce expression of Ang-1 and potentially models activities in patients with low or heterogeneous Ang-1 expression.[43,44] In this experiment, Tie2.1-hexamer was able to suppress LPS-induced vascular leakage, whereas anti-VEGF or anti-Ang-2 (nevascumab) did not (Fig. 3c). Permeability in the Miles assays was reduced to a
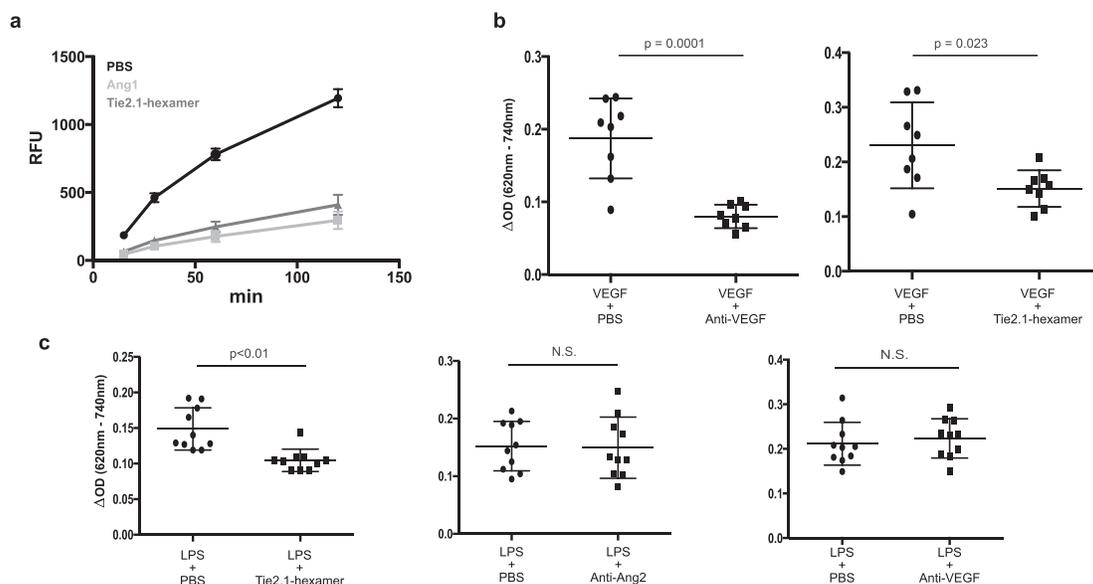
Figure 3. Tie2 agonists reduce the permeability of monolayers and murine vasculature. (a) HUVECs were grown to confluency in Transwell plates, transferred to serum-free basal medium for 16 hours, and treated with the indicated agonists for 30 minutes. FITC-labeled dextran was added to the wells, and passage through the cellular monolayer was analyzed over time. Balb/C mice were administered Evans Blue dye intravenously followed by a combination of an inducer of edema (LPS or VEGF) and a drug or negative control intradermally into the ears. Thirty minutes following intradermal injection the mice were sacrificed; the dye was extracted from the ears and quantified spectrophotometrically. (b) Activity of anti-VEGF and Tie2.1-hexamer in response to VEGF-induced edema. (c) Activity of Tie2.1-hexamer, anti-Ang-2, and anti-VEGF in response to LPS-induced edema. Data shown in (a) ($n = 3$) and in (b) and (c) ($n = 8$–10) are mean $\pm$ SD.

level similar to what is seen in mice not treated with inducers of vascular leak (Supplementary Fig. S4). Collectively, these data support the hypothesis that, under appropriate conditions, direct Tie2 agonism is functionally differentiated from both VEGF and Ang-2 inhibition.

Pharmacokinetic Behavior of Tie2.1-Hexamer

Given the importance of infrequent dosing in ensuring patient compliance, we evaluated the exposure of the Tie2.1-hexamer following intravitreal administration into cynomolgus monkeys (Fig. 4a). Following a single 2-mg/eye bilateral intravitreal injection, the hexamer showed durable vitreal ($t_{1/2}$ of 5 days) and aqueous ($t_{1/2}$ of 4.1 days) exposure. Maximum exposure (C_{max}) of the Tie2.1-hexamer was approximately 200-fold lower in the serum than the vitreous and cleared more rapidly ($t_{1/2}$ of 2.3 days). Routine clinical ophthalmic examinations (slit-lamp biomicroscopy and indirect ophthalmoscopy) were performed during this study, and intravitreal administration of Tie2.1-hexamer was well tolerated. Concentrations achieved in all three compartments (Fig. 4a) were greater than 10-fold higher than the threshold required to drive activity based on in vitro potency assays (Fig. 1c).

Pharmacodynamics of Tie2.1-Hexamer in Cynomolgus Monkeys

We sought to identify biomarkers of Tie2 activity both to validate the function of the Tie2.1-hexamer in monkeys following intravitreal administration and to set the stage for eventual validation in human clinical trials. Primary human retinal microvascular endothelial cells were treated with the Tie2.1-hexamer or a buffer control for 4 hours, and gene expression profiles were assessed by RNA-sequencing. A total of 57 genes showed significant upregulation and 102 genes were suppressed, including *PDGFB*, *PGF*, *ESM1*, and *ANGPT2*, the gene encoding for Ang-2 (Figs. 4b, 4c; Supplementary Table S1). To explore Ang-2 as a potential pharmacodynamic biomarker, we assessed the monkey plasma samples for Ang-2 levels following intravitreal administration of the Tie2 agonist or non-binding control. Although a non-binding control induced minimal variation in Ang-2 concentration, the Tie2.1-hexamer transiently suppressed plasma Ang-2 levels for at least 7 days following administration, followed by complete recovery by day 21 (Fig. 4d). These data suggest that Tie2.1-hexamer was active in the cynomolgus monkeys and Ang-2 could potentially serve as a pharmacodynamic biomarker for monitoring Tie2 target engagement.
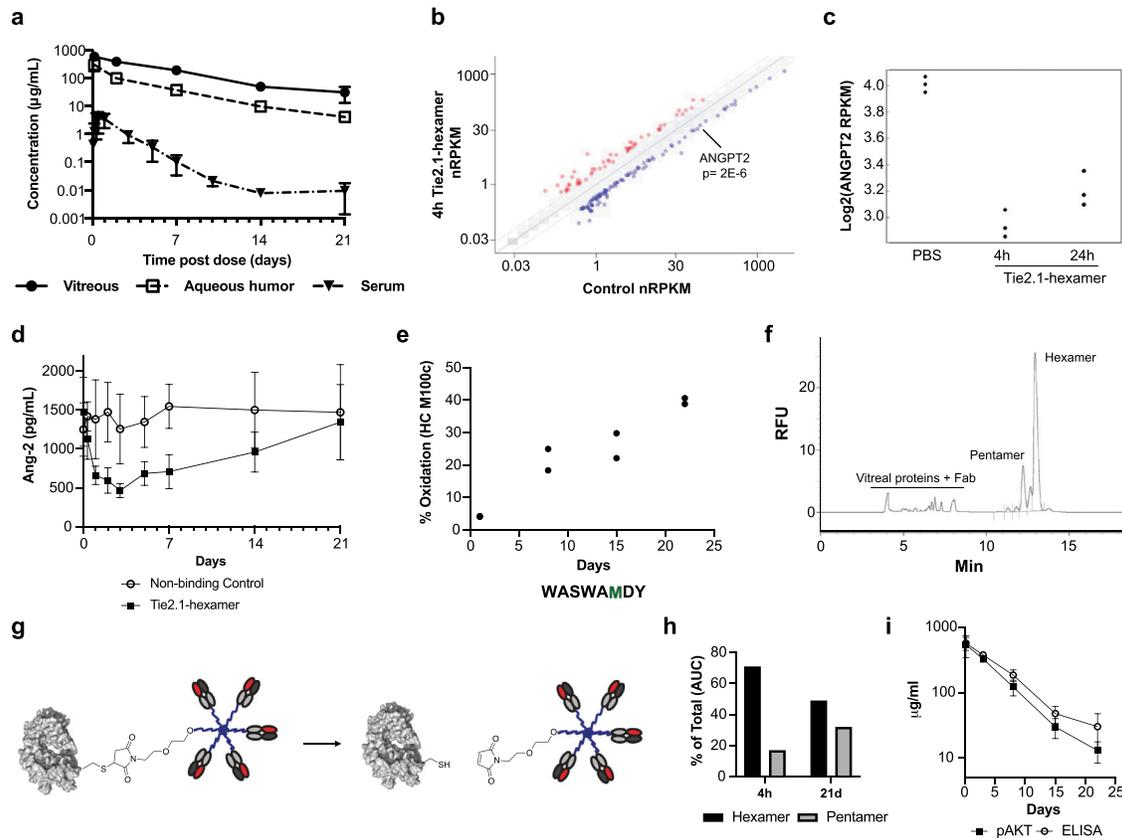
Figure 4. In vivo exposure, activity, and stability of Tie2.1-hexamer. (a) Pharmacokinetic profiles of Tie2.1-hexamer following 2-mg/eye bilateral intravitreal injection into male cynomolgus monkeys. (b) RNA-sequencing analysis of gene expression levels in primary human retinal microvascular endothelial cells treated with 10 μg/mL of Tie2.1-hexamer or PBS for 4 hours compared to control. (c) Ang-2 RNA-sequencing expression levels in human retinal microvascular endothelial cells treated with PBS or 10 μg/mL of Tie2.1-hexamer for 4 hours or 24 hours. (d) ELISA analysis of Ang-2 levels in monkey plasma following treatment with Tie2.1-hexamer or a non-binding control. (e) LC-MS/MS analysis of Tie2.1-hexamer isolated from monkey vitreous 4 hours to 21 days following administration. Sequence of the relevant peptide is shown with the oxidized residue in *green*. (f) CE–SDS–LIF electropherogram of monkey vitreous isolated 4 hours following intravitreal injection of Tie2.1-hexamer. (g) Schematic showing retro-Michael decomposition of Tie2.1-hexamer into a Tie2.1-pentamer and Fab. (h) CE–SDS–LIF quantitation of Tie2.1-hexamer and Tie2.1-pentamer in monkey vitreous isolated 4 hours and 21 days following intravitreal administration of Tie2.1-hexamer. (i) Concentrations of Tie2.1-hexamer in monkey vitreous determined by pAKT activation versus ELISA signal. Data shown in (a), (d), and (i) are mean ± SD. *Error bars* are not included if they are less than the size of the marker.

In Vivo Stability of the Tie2.1-Hexamer

As the proposed therapeutic format was complex and there is somewhat limited knowledge of the impact of vitreal stresses on protein stability, we characterized the biotransformation of the Tie2.1-hexamer recovered from the monkey vitreous. Vitreal samples were digested by trypsin and analyzed by liquid chromatography with tandem mass spectrometry (LC-MS-MS), which revealed progressive oxidation at HC M100c culminating at 40% by day 21 (Fig. 4e). To understand the functional impact of this oxidation, we treated the Tie2.1-hexamer with hydrogen peroxide to drive fractional oxidation, and monitored the activity of the resulting species. Treatment resulting in 65% oxidation of M100c (and no other detectable modifications),

reduced the potency in the pAKT assay by approximately threefold and reduced the maximum signal by ~10% (Supplementary Fig. S5). A holistic view of the structure of the hexamer was undertaken by CE–SDS–LIF.[45] The large size of the hexamer, coupled with the low protein abundance in the vitreous humor, allowed sensitive detection and electrophoretic separation of the PEG conjugates from endogenous protein (Fig. 4f). The analyses revealed evidence of degradation of the hexamer predominantly to Tie2.1-pentamer and Tie2.1-tetramer, progressing from 71% hexamer on day 1 to 49% hexamer on day 22 (Figs. 4g, 4h). To understand the combined impact of oxidation and deconjugation, we characterized the ex vivo specific activity of material recovered from the vitreous using the HUVEC pAKT functional cell-based assay to assess total

activity, and ELISA (vs. total Fab) to determine concentration (Fig. 4i). Four hours following dosing we recovered 94% of the activity predicted using our ELISA quantitation; by day 22, it was reduced to 47% of the anticipated activity ($P < 0.01$).

Generation and Functional Assessment of Stabilized Tie2.1-Hexamers

We sought to mitigate the molecular changes to Tie2.1-hexamer that occurred in vivo and were detrimental to its activity. To eliminate any potential effect associated with HC M100c oxidation, we scanned through potential M100c mutations and assessed binding to Tie2. We found that a M100cF mutation exhibits modestly enhanced binding to Tie2 and eliminates the observed site of oxidation (Supplementary Fig. S6).

Tie2.1-hexamer was generated by adding the Tie2.1 Fab containing a C-terminal cysteine to a hexameric PEG capped with maleimide moieties. Because the exposed cysteine conjugates can undergo reverse Michael reactions (Fig. 4g), we suspected that the observed degradation of the Tie2.1-hexamer could be caused by deconjugation of the Tie2.1 Fab.[46] Previous studies of thiol-maleimide antibody–drug conjugates have shown that strategically placed cysteine mutants can conjugate effectively with limited deconjugation.[47] Based on the cysteine mutants reported to form stable conjugates, we generated a panel of Tie2.1 M100cF Fabs carrying a single cysteine replacement at different sites in either heavy chain or light chain and conjugated them to the hexamer PEG scaffold. The resulting conjugates were tested for their stability and activity. We identified two mutants, HC T209C and LC T206C, that gave rise to PEG conjugates with improved stability in vitro and substantially retained activity (Supplementary Fig. S7). In cultured HUVECs, all three versions of the Tie2.1-hexamer M100cF Fabs, conjugated through the C-terminal cysteine, HC T209C, or LC T206C, promoted changes in cortical actin and adherens junctions and similarly attenuated leakage through serum-starved monolayers (Supplementary Figs. S8, S9).

Next, we assessed in vivo stability and activity comparing three versions of the Tie2.1-hexamers. Following 2-mg/eye intravitreal administration to cynomolgus monkeys, all of the hexamers showed similar vitreal and aqueous exposures (Fig. 5a). Assessment of the extracted vitreous by CE–SDS–LIF confirmed partial degradation of the C-terminal conjugate which was partially or wholly mitigated by alternative conjugation sites (Fig. 5b). We assessed ex vivo specific activity of the vitreous samples using the combination of HUVEC pAKT cell-based assay and ELISA. Unlike the parental Tie2.1-hexamer, the three Tie2.1 M100cF hexamers showed no significant loss in activity over time (Fig. 5c), confirming that oxidation at M100c was the major biotransformation driving activity loss. Finally, we confirmed that the most stable agonist, conjugated via T209C, was active in the Miles assay (Supplementary Fig. S10).

Discussion

Following substantial preclinical evidence highlighting Tie2 as a promising target for the treatment of diabetic macular edema, various strategies have been explored in the clinic that indirectly activate the pathway by blocking inhibitory factors upstream (Ang-2) or downstream (VE-PTP) of kinase activation.[26,49–51] Although the Time2b (AKB-9778/VE-PTP) and RUBY/ONYX (nesvacumab/Ang-2) trials failed to demonstrate robust clinical benefit, the recent approval of faricimab supports that the Ang/Tie2 pathway is an important therapeutic axis in ocular disease and suggests that determining the details of how the pathway is engaged and developing an appropriate clinical design will be important in defining patients' responses. Given the combination of preclinical and clinical validation of the pathway, we explored approaches to drive enhanced Tie2 signaling beyond what might be achievable by removing negative regulators.

To better understand the potential impact of direct pathway activation, we compared Tie2 agonists to VEGF or Ang-2 inhibitors. In the modified Miles assay, VEGF-induced vascular leak was reduced by either anti-VEGF or our Tie2 agonists (Fig. 3b); however, vascular leak induced by LPS was mitigated only by direct Tie2 agonism (Fig. 3c). We hypothesize that anti-VEGF agents are unable to mitigate the more complex mixture of cytokines induced by LPS. Additionally, LPS both reduces Ang1 and drives β1 integrin expression, potentially explaining why anti-Ang-2 is ineffective in this model.[44,52] A potential risk of this approach is that elevated levels of Ang-2 present in the eyes of patients with DME could compete with the direct agonist for activity. We show such inhibition can occur, but at Ang-2 levels reported to be present in the eyes of patients with DME[16] it is readily overcome by levels of Tie2.1-hexamer durably achieved in the eye (Supplementary Fig. S2). Collectively, these studies highlight ways in which Tie2 agonism differentiates itself from established therapeutic approaches, but the complexity of human disease is challenging to model preclinically. Acute murine models likely fail to fully
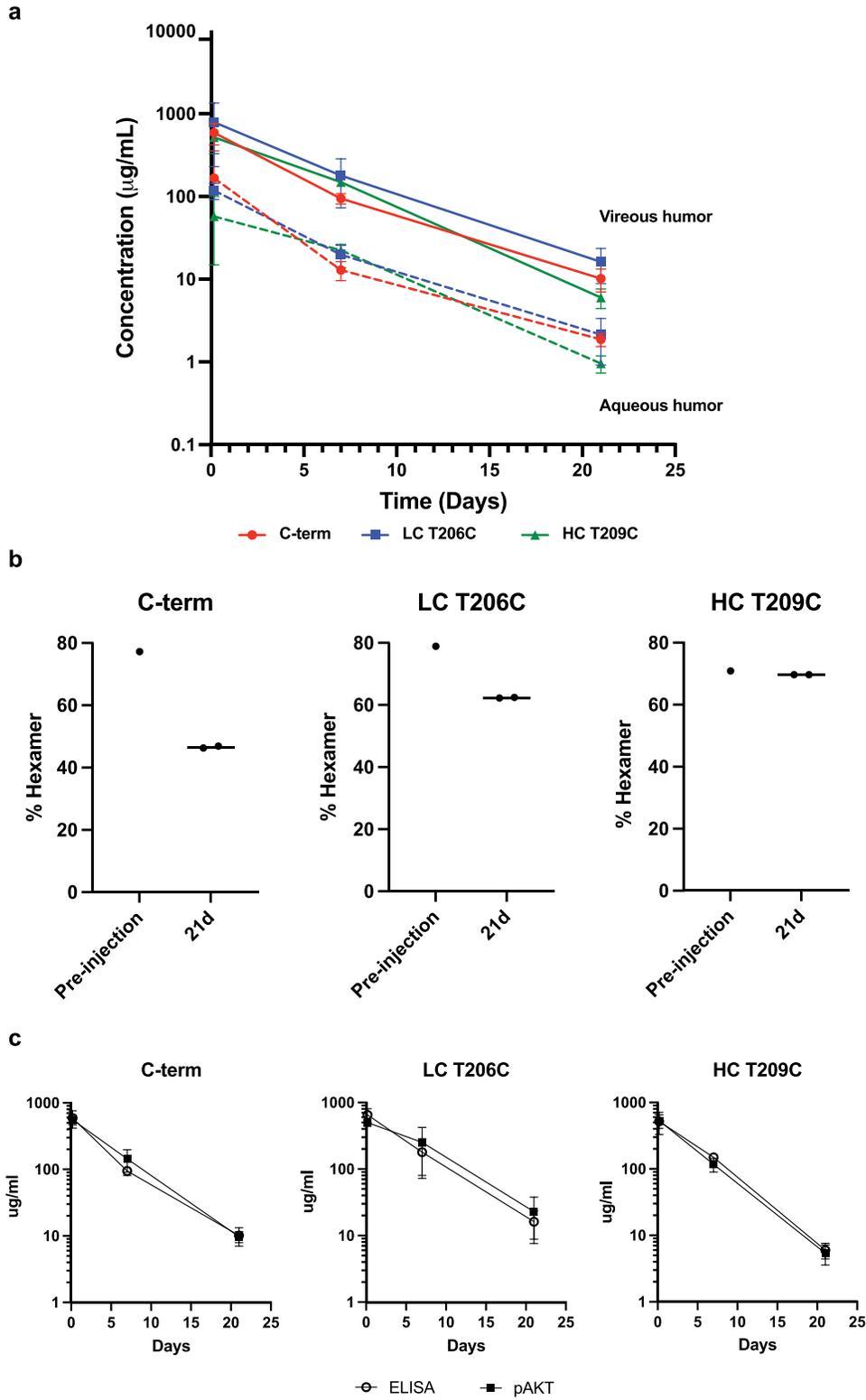
Figure 5. In vivo exposure and stability of stabilized Tie2.1-hexamers. (a) Pharmacokinetic profiles of Tie2.1-hexamers following 2-mg/eye bilateral intravitreal injection into male cynomolgus monkeys. (b) CE–SDS–LIF analysis of injection solutions and monkey vitreous 21 days following the intravitreal injection of the indicated Tie2.1-hexamers. (c) Concentration of Tie2.1-hexamers in monkey vitreous as determined by ELISA or from downstream activation of pAKT aligned to a standard curve. Data shown in (a) and (c) are mean $\pm$ SD.

recapitulate the physiology of slowly developing DME-driven edema. VEGF signaling, which is typically suppressed in patients treated with anti-VEGF therapies, is reported to both indirectly activate Tie2 and promote shedding of its extracellular domain.[53,54]

A further consideration is that, although our preclinical activities show substantial single-agent activity for the Tie2-hexamer, anti-VEGF agents are broadly effective as the standard of care in DME and are anticipated to remain a platform for additional agents. Still, a substantial number of patients do not achieve optimal vision even with monthly intravitreal injections of anti-VEGF. Patients with chronic persistent retinal fluid may develop irreversible vision loss if left untreated or inadequately treated. For example, in the RISE/RIDE phase III study of ranibizumab, patients who crossed over and received treatment after 2 years of sham injections showed similar improvement on optical coherence tomography but only gain half of the vision as those treated early.[48] Although the need for improvements over the current standard of care is clear, the clinical validation of a combination therapy on top of anti-VEGF (e.g., anti-VEGF + Tie2 agonist) will require any new molecule to demonstrate significantly improved efficacy as measured by best-corrected visual acuity in a head-to-head clinical study. We hypothesize that patients with strong responses to anti-VEGF alone may have a limited window for visual improvement. This cap on activity could partially mask Tie2-driven improvements in patients requiring additional intervention. Lead-in treatments with anti-VEGF may help identify patients with DME who are likely to have persistent edema with concomitant vision loss with anti-VEGF alone and would be more likely to benefit from the addition of a second therapeutic agent.

In addition to the therapeutic implications, our current work also revealed important molecular insights into designing an optimal Tie2 agonist. Signaling duration is a critical consideration for agonistic agents. Activation of receptor tyrosine kinases can lead to their internalization, resulting in diminished signaling with time.[55] In our study, we investigated two types of Tie2 agonists, the biparatopic Tie2.1.38 and Tie2.1-hexamer. Compared with Tie2.1-hexamer, Tie2.1.38 triggered a greater degree of Tie2 downregulation, resulting in transient Tie2 signaling. We found that multi-armed PEG scaffolds with more binding arms and with shorter distances between the binding arms exhibited greater activity. Interestingly, subtle variations of geometry influenced activity, with LC T206C showing the greatest activity. Tie2.1-hexamer exhibited a bell-shaped dose response in vitro, which may limit its therapeutic activity at high concentrations. Extrapolation of these in vitro differences to

relevant biological activities is uncertain. The Tie2.1-hexamer must diffuse from the vitreous through the retina to reach the target cells, so we anticipate lower local concentrations than were observed in the vitreous of Figure 4. Furthermore, the strength of Tie2 signaling necessary to improve vision is undefined. The reported Tie2.1-Fab has a weak ($\sim$3 µM) monovalent affinity at 37°C (Supplementary Fig. S1), whereas in the hexavalent format we observed avidity driven potency in the picomolar range (Figs. 1C, 1D). Higher affinity binders might shift the inhibitory response to lower concentrations and narrow the activity window, a feature potentially incompatible with the demand for infrequent high-dose intravitreal injections.

Additional characteristics of the molecule also support less frequent administration. Despite the low monovalent activity, activity is seen at doses as low as 100 ng/mL in vitro (Figs. 1C, 1D) and in monkey serum (Figs. 4a, 4d), presumably resulting from strong avidity of the hexameric molecule. The observed vitreal C_{max} was nearly 1 mg/mL (Figs. 4a, 5a) with confirmed ex vivo activity (Figs. 4i, 5c), suggesting that the molecule may be active over a range of more than three orders of magnitude. Furthermore, the larger hydrodynamic radius (R_h) slows vitreal clearance of the conjugate; the measured half-life in monkey (5 days) is approximately twofold longer than that of anti-VEGF therapeutics (ranibizumab, 2.3 days; bevacizumab, 2.9 days; aflibercept, 3.6 days), enabling sustained vitreal exposure within the therapeutic window.[56] Finally, engineering to remove both oxidation and deconjugation liabilities results in a molecule that maintains its activity over time in the monkey vitreous.

In summary, we have described the discovery of a direct Tie2 agonist with desirable features for infrequent ocular administration. Given their unique molecular design and mechanism of action, Tie2.1-hexamers are promising candidates for further clinical development.

Acknowledgments

Disclosure: **N.J. Agard**, Genentech, Inc. (E, I, P); **G. Zhang**, Genentech, Inc. (E, I, P); **J. Ridgeway**, Genentech, Inc. (E, I); **D.M. Dicara**, Genentech, Inc.

(E, I, P); **P.Y. Chu**, Genentech, Inc. (E, I); **R. Ohri**, Genentech, Inc. (E, I); **S. Sanowar**, Genentech, Inc. (E, I, P); **J.-M. Vernes**, Genentech, Inc. (E, I); **H. Chi**, Genentech, Inc. (E, I); **J. Zhang**, Genentech, Inc. (E, I); **E. Holz**, Genentech, Inc. (E, I); **M. Paluch**, Genentech, Inc. (E, I); **G. He**, Genentech, Inc. (E, I); **Y. Benson**, Genentech, Inc. (E, I); **J. Zhang**, Genentech, Inc. (E, I); **P. Chan**, Genentech, Inc. (E, I); **N. Tang**, Genentech, Inc. (E, I); **P. Javale**, Genentech, Inc. (E, I); **B. Wilson**, Genentech, Inc. (E, I); **K. Barrett**, Genentech, Inc. (E, I); **R.K. Rowntree**, Genentech, Inc. (E, I); **J. Hang**, Genentech, Inc. (E, I, P); **Y.G. Meng**, Genentech, Inc. (E, I); **P. Hass**, Genentech, Inc. (E, I, P); **G. Fuh**, Genentech, Inc. (E, I); **R. Piskol**, Genentech, Inc. (E, I); **V. Bantseev**, Genentech, Inc. (E, I); **K.M. Loyet**, Genentech, Inc. (E, I); **J.C. Tran**, Genentech, Inc. (E, I); **C. Wu**, Genentech, Inc. (E, I); **V.B. Indjeian**, Genentech, Inc. (E, I); **V. Shivva**, Genentech, Inc. (E, I, P); **M. Yan**, Genentech, Inc. (E, I, P)

* NJA and GZ contributed equally to this work.

References

1. Zimmet P, Alberti KG, Magliano DJ, Bennett PH. Diabetes mellitus statistics on prevalence and mortality: facts and fallacies. *Nat Rev Endocrinol*. 2016;12(10):616–622.

2. Centers for Disease Control and Prevention. National Diabetes Statistics Report: estimates of diabetes and its burden in the United States. Available at: https://www.cdc.gov/diabetes/data/statistics-report/index.html#:~:text=Suggested%20Citation&text=National%20Diabetes%20Statistics%20Report%2C%202020.,Health%20and%20Human%20Services%3B%202020. Accessed September 28, 2022.

3. Zhang X, Saaddine JB, Chou CF, et al. Prevalence of diabetic retinopathy in the United States, 2005–2008. *JAMA*. 2010;304(6):649–656.

4. Kempen JH, O'Colmain BJ, Leske MC, et al. The prevalence of diabetic retinopathy among adults in the United States. *Arch Ophthalmol*. 2004;122(4):552–563.

5. Yau JWY, Rogers SL, Kawasaki R, et al. Global prevalence and major risk factors of diabetic retinopathy. *Diabetes Care*. 2012;35(3):556–564.

6. Park SJ, Ahn S, Woo SJ, Park KH. Extent of exacerbation of chronic health conditions by visual impairment in terms of health-related quality of life. *JAMA Ophthalmol*. 2015;133(11):1267–1275.

7. Bhagat N, Grigorian RA, Tutela A, Zarbin MA. Diabetic macular edema: pathogenesis and treatment. *Surv Ophthalmol*. 2009;54(1):1–32.

8. Romero-Aroca P, Baget-Bernaldiz M, Pareja-Rios A, Lopez-Galvez M, Navarro-Gil R, Verges R. Diabetic macular edema pathophysiology: vasogenic versus inflammatory. *J Diabetes Res*. 2016;2016:2156273.

9. Schröder S, Palinski W, Schmid-Schönbein GW. Activated monocytes and granulocytes, capillary nonperfusion, and neovascularization in diabetic retinopathy. *Am J Pathol*. 1991;139(1):81–100.

10. Singh RP, Elman MJ, Singh SK, Fung AE, Stoilov I. Advances in the treatment of diabetic retinopathy. *J Diabetes Complications*. 2019;33(12):107417.

11. Gupta N, Mansoor S, Sharma A, et al. Diabetic retinopathy and VEGF. *Open Ophthalmol J*. 7(1):4–10.

12. Nguyen QD, Brown DM, Marcus DM, et al. Ranibizumab for diabetic macular edema. *Ophthalmology*. 2012;119(4):789–801.

13. Weiss M, Sim DA, Herold T, et al. Compliance and adherence of patients with diabetic macular edema to intravitreal anti-vascular endothelial growth factor therapy in daily practice. *Retina*. 2018;38(12):2293–2300.

14. Campochiaro PA, Marcus DM, Awh CC, et al. The port delivery system with ranibizumab for neovascular age-related macular degeneration. *Ophthalmology*. 2019;126(8):1141–1154.

15. Sun JK, wen Wang P, Taylor S, Haskova Z. Durability of diabetic retinopathy improvement with as-needed ranibizumab open-label extension of RIDE and RISE studies. *Ophthalmology*. 2019;126(5):712–720.

16. Regula JT, von Leithner PL, Foxton R, et al. Targeting key angiogenic pathways with a bispecific CrossMAb optimized for neovascular eye diseases. *EMBO Mol Med*. 2016;8(11):1265–1288.

17. Sahni J, Patel SS, Dugel PU, et al. Simultaneous inhibition of angiopoietin-2 and VEGF-A with faricimab in diabetic macular edema: BOULEVARD Phase 2 randomized trial. *Ophthalmology*. 2019;126(8):1155–1170.

18. Maisonpierre PC, Suri C, Jones PF, et al. Angiopoietin-2, a natural antagonist for Tie2 that disrupts in vivo angiogenesis. *Science*. 1997;277(5322):55–60.

19. Hakanpaa L, Sipila T, Leppanen VM, et al. Endothelial destabilization by angiopoietin-2 via integrin β1 activation. *Nat Commun*. 2015;6(1):5962.

20. Watanabe D, Suzuma K, Suzuma I, et al. Vitreous levels of angiopoietin 2 and vascular endothelial

growth factor in patients with proliferative diabetic retinopathy. *Am J Ophthalmol*. 2005;139(3):476–481.

21. Fiedler U, Augustin HG. Angiopoietins: a link between angiogenesis and inflammation. *Trends Immunol*. 2006;27(12):552–558.

22. Khan M, Aziz AA, Shafi NA, Abbas T, Khanani AM. Targeting angiopoietin in retinal vascular diseases: a literature review and summary of clinical trials involving faricimab. *Cells*. 2020;9(8):1869.

23. Wykoff CC, Abreu F, Adamis AP, et al. Efficacy, durability, and safety of intravitreal faricimab with extended dosing up to every 16 weeks in patients with diabetic macular oedema (YOSEMITE and RHINE): two randomised, double-masked, phase 3 trials. *Lancet*. 2022;399(10326):741–755.

24. Wells JA. Faricimab in DME: 2 year data of the YOSEMITE/RHINE phase 3 studies. Paper presented at Angiogenesis, Exudation, and Degeneration 2022–Virtual Edition, February 12, 2022.

25. Campochiaro PA, Sophie R, Tolentino M, et al. Treatment of diabetic macular edema with an inhibitor of vascular endothelial-protein tyrosine phosphatase that activates Tie2. *Ophthalmology*. 2015;122(3):545–554.

26. Shen J, Frye M, Lee BL, et al. Targeting VE-PTP activates TIE2 and stabilizes the ocular vasculature. *J Clin Invest*. 2014;124(10):4564–4576.

27. Hussain RM, Neiweem AE, Kansara V, Harris A, Ciulla TA. Tie-2/Angiopoietin pathway modulation as a therapeutic strategy for retinal disease. *Expert Opin Investig Drugs*. 2019;28(10):861–869.

28. Edelman GM, Cunningham BA, Gall WE, Gottlieb PD, Rutishauser U, Waxdal MJ. The covalent structure of an entire γG immunoglobulin molecule. *Proc Natl Acad Sci USA*. 1969;63(1):78–85.

29. Wu TT, Kabat EA. An analysis of the sequences of the variable regions of Bence Jones proteins and myeloma light chains and their implications for antibody complementarity. *J Exp Med*. 1970;132(2):211–250.

30. Bostrom J, Fuh G. Design and construction of synthetic phage-displayed Fab libraries. *Methods Mol Biol*. 2009;562:17–35.

31. Junutula JR, Raab H, Clark S, et al. Site-specific conjugation of a cytotoxic drug to an antibody improves the therapeutic index. *Nat Biotechnol*. 2008;26(8):925–932.

32. Wu TD, Nacu S. Fast and SNP-tolerant detection of complex variants and splicing in short reads. *Bioinformatics*. 2010;26(7):873–881.

33. Law CW, Chen Y, Shi W, Smyth GK. voom: precision weights unlock linear model analysis tools for RNA-seq read counts. *Genome Biol*. 2014;15(2):R29.

34. Ritchie ME, Phipson B, Wu D, et al. limma powers differential expression analyses for RNA-sequencing and microarray studies. *Nucleic Acids Res*. 2015;43(7):e47.

35. Srinivasan K, Friedman BA, Larson JL, et al. Untangling the brain's neuroinflammatory and neurodegenerative transcriptional responses. *Nat Commun*. 2016;7(1):11295.

36. Salas-Solano O, Tomlinson B, Du S, Parker M, Strahan A, Ma S. Optimization and validation of a quantitative capillary electrophoresis sodium dodecyl sulfate method for quality control and stability monitoring of monoclonal antibodies. *Anal Chem*. 2006;78(18):6583–6594.

37. Michels DA, Brady LJ, Guo A, Balland A. Fluorescent derivatization method of proteins for characterization by capillary electrophoresis- sodium dodecyl sulfate with laser-induced fluorescence detection. *Anal Chem*. 2007;79(15):5963–5971.

38. Kim KT, Choi HH, Steinmetz MO, et al. Oligomerization and multimerization are critical for angiopoietin-1 to bind and phosphorylate Tie2. *J Biol Chem*. 2005;280(20):20126–20131.

39. Yang Y, Yeh SH, Madireddi S, et al. Tetravalent biepitopic targeting enables intrinsic antibody agonism of tumor necrosis factor receptor superfamily members. *Mol Cell Ther*. 2019;11(6):996–1011.

40. Saharinen P, Eklund L, Miettinen J, et al. Angiopoietins assemble distinct Tie2 signalling complexes in endothelial cell–cell and cell–matrix contacts. *Nat Cell Biol*. 2008;10(5):527–537.

41. Kim I, Kim JH, Moon SO, Kwak HJ, Kim NG, Koh GY. Angiopoietin-2 at high concentration can enhance endothelial cell survival through the phosphatidylinositol 3′-kinase/Akt signal transduction pathway. *Oncogene*. 2000;19(39):4549–4552.

42. Radu M, Chernoff J. An in vivo assay to test blood vessel permeability. *J Vis Exp*. 2013;73:e50062.

43. Tarr JM, Kaul K, Chopra M, Kohner EM, Chibber R. Pathophysiology of diabetic retinopathy. *ISRN Ophthalmol*. 2013;2013:343560.

44. Mofarrahi M, Nouh T, Qureshi S, Guillot L, Mayaki D, Hussain SNA. Regulation of angiopoietin expression by bacterial lipopolysaccharide. *Am J Physiol Lung Cell Mol Physiol*. 2008;294(5):L955–L963.

45. Zhu Z, Lu JJ, Liu S. Protein separation by capillary gel electrophoresis: a review. *Anal Chim Acta*. 2012;709:21–31.

46. Zheng K, Chen Y, Wang J, et al. Characterization of ring-opening reaction of succinimide linkers in ADCs. *J Pharm Sci*. 2018;108(1):133–141.

47. Ohri R, Bhakta S, Fourie-O'Donohue A, et al. High-throughput cysteine scanning to identify stable antibody conjugation sites for maleimide- and disulfide-based linkers. *Bioconjug Chem*. 2018;29(2):473–485.

48. Brown DM, Nguyen QD, Marcus DM, et al. Long-term outcomes of ranibizumab therapy for diabetic macular edema: the 36-month results from two phase III trials. *Ophthalmology*. 2013;120(10):2013–2022.

49. Campochiaro PA, Khanani A, Singer M, et al. Enhanced benefit in diabetic macular edema from AKB-9778 Tie2 activation combined with vascular endothelial growth factor suppression. *Ophthalmology*. 2016;123(8):1722–1730.

50. Han S, Lee SJ, Kim KE, et al. Amelioration of sepsis by TIE2 activation–induced vascular protection. *Sci Transl Med*. 2016;8(335):335ra55.

51. Nguyen QD, Heier JS, Do DV, et al. The Tie2 signaling pathway in retinal vascular diseases: a novel therapeutic target in the eye. *Int J Retin Vitreous*. 2020;6(1):48.

52. Hsu RYC, Chan CHF, Spicer JD, et al. LPS-induced TLR4 signaling in human colorectal cancer cells increases $\beta 1$ integrin-mediated cell adhesion and liver metastasis. *Cancer Res*. 2011;71(5):1989–1998.

53. Singh H, Milner CS, Hernandez MMA, Patel N, Brindle NPJ. Vascular endothelial growth factor activates the Tie family of receptor tyrosine kinases. *Cell Signal*. 2009;21(8):1346–1350.

54. Findley CM, Cudmore MJ, Ahmed A, Kontos CD. VEGF induces Tie2 shedding via a phosphoinositide 3-kinase/Akt–dependent pathway to modulate Tie2 signaling. *Arterioscler Thromb Vasc Biol*. 2007;27(12):2619–2626.

55. Bogdanovic E, Nguyen VPKH, Dumont DJ. Activation of Tie2 by angiopoietin-1 and angiopoietin-2 results in their release and receptor internalization. *J Cell Sci*. 2006;119(17):3551–3560.

56. Crowell SR, Wang K, Famili A, et al. Influence of charge, hydrophobicity, and size on vitreous pharmacokinetics of large molecules. *Transl Vis Sci Technol*. 2019;8(6):1.